ISSN: **2229-7359** Vol. 11 No. 18s, 2025

https://www.theaspd.com/ijes.php

# Renoprotective Effects Of Novel Simvastatin Derivatives (A1 And A2) In A Rat Model Of Induced Hypercholesterolemia: Biochemical And Histopathological Evaluation

Amaal H. Sheaa<sup>1</sup>, Sameerah Ahmed Zearah<sup>2</sup>, Abass F. Abass<sup>2</sup>

pgs.amaal.hussein@uobasrah.edu.iq sameera.zearah@uobasrah.edu.iq abbas.f.abbas@uobasrah.edu.iq

<sup>1</sup>Department of Medical Laboratory Techniques, College of Health and Medical Technologies, Southern Technical University, Basrah, Iraq.

<sup>2</sup>Department of Chemistry, College of Science, University of Basrah, Basrah, Iraq.

ABSTRACT. This study explores the synthesis, structural characterization, and evaluation of renal safety of two novel simvastatin ester derivatives (A1 and A2), prepared via a green one-pot esterification method using triphenylohosphine (Ph<sub>3</sub>P), iodine (I<sub>2</sub>), and 4-dimethylaminopyridine (DMAP). Structural confirmation was achieved using FT-IR, <sup>1</sup>H-NMR, <sup>13</sup>C-NMR, and mass spectrometry, with key fragmentation patterns supporting successful derivatization. The nephrological safety and potential therapeutic effects of the synthesized compounds were assessed in vivo using a rat model of cholesterol-induced hypercholesterolemia. Biochemical markers of kidney function, including serum creatinine, urea were analyzed alongside detailed histopathological examinations. Treatment with A1 and A2 led to a significant improvement in renal parameters compared to the hypercholesterolemic control group, with A1 showing superior efficacy in reducing urea and BUN levels, while A2 demonstrated better histological preservation of renal architecture. Both derivatives outperformed the reference drug simvastatin in terms of nephrotoxicity mitigation. The findings support the hypothesis that structural modification of simvastatin via esterification with short-chain fatty acids may improve its renal safety profile without compromising its lipid-lowering potential. These results contribute to the growing interest in organ-targeted statin derivatives as safer alternatives in long-term cardiovascular and metabolic disease management.

**KEYWORDS:** Simvastatin derivatives, Esterification, Kidney function, Histopathology, Lipid-lowering agents Hypercholesterolemia.

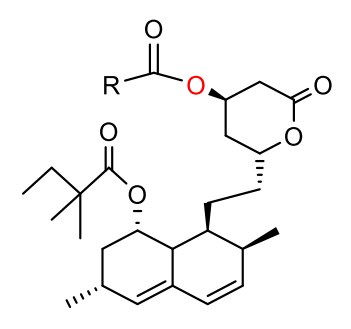
# INTRODUCTION

Over the past few decades, the global health landscape has been reshaped by profound lifestyle changes, particularly the growing prevalence of sedentary behavior and diets rich in calories and saturated fats. These trends have significantly contributed to the rise in hypercholesterolemia and dyslipidemia, both of which are firmly established as major risk factors for cardiovascular disease (CVD), the leading cause of death worldwide(Safapoor et al., n.d.). A key player in this pathology is the elevated concentration of low-density lipoprotein cholesterol (LDL-C), which drives the development of atherosclerosis. This has led to a pressing need for effective lipid-lowering therapies that go beyond mere tolerability to ensure long-term safety, patient compliance, and minimal systemic toxicity. Statins have become a cornerstone in the management and prevention of CVD due to their ability to inhibit the rate-limiting enzyme 3-hydroxy-3-methylglutaryl coenzyme A reductase (HMG-CoA reductase) (Su et al., 2016). Among them, simvastatin, semisvnthetic derivative of lovastatin-stands out for its excellent clinical efficacy and pharmacokinetic profile. However, statins are not without challenges. Limitations such as low aqueous solubility, inconsistent bioavailability, and dose-dependent adverse effects have motivated ongoing efforts to enhance their performance through

ISSN: **2229-7359** Vol. 11 No. 18s, 2025

https://www.theaspd.com/ijes.php

structural modifications (Sadowska et al., 2024). Esterification has emerged as a compelling strategy in this regard. Within the realm of bioorganic and medicinal chemistry, esterifying hydroxyl-bearing pharmaceuticals has proven useful in improving lipid solubility, enhancing metabolic stability, mitigating side effects, and enabling controlled drug release. Simvastatin, with its accessible hydroxyl functional group, is a prime candidate for such chemical tailoring. By incorporating small carboxylic acids like acetic and butanoic acid, it is possible to generate novel ester derivatives of simvastatin with potentially superior physicochemical and pharmacological profiles (Abd-Elghany et al., 2023). Achieving this through green chemistry is particularly appealing, as traditional esterification methods often require harsh conditions-such as strong acids, elevated temperatures, or dehydrating agents-that may compromise molecular integrity(Fernandes et al., 2020; Sabah Al-Obaidi et al., n.d.). In contrast, the triphenylphosphine/iodine (Ph<sub>3</sub>P/I<sub>2</sub>) system, in the presence of a catalytic amount of 4-dimethylaminopyridine (DMAP), offers a mild, high-yield, and environmentally considerate route for ester bond formation (Sardarian et al., 2009). This one-pot methodology simplifies synthesis, reduces reaction time, and limits by-product formation-making it ideal for pharmaceutical applications and scalable drug development. In this study, we describe the synthesis and characterization of two novel simvastatin esters-an acetate and a butanoate derivative-using this green one-pot esterification method, figure 1. Structural confirmation was achieved via FT-IR, <sup>1</sup>H-NMR, <sup>13</sup>C-NMR, and ESI-MS, with emphasis on identifying key fragmentation patterns indicative of successful derivatization. Beyond their lipidlowering potential, special attention was given to evaluating the renal safety of these derivatives. Kidney toxicity remains a critical concern in the long-term use of many statins, especially in patients with pre-existing renal impairment or those requiring chronic therapy. Therefore, the current study also improved renal safety, thus supporting their candidacy as safer and more effective alternatives in dyslipidemia management.



 $R= CH_3, CH_3CH_2$ 

Figure 1: General structure of new compounds

### **EXPERIMENTAL**

#### Chemicals Material

Simvastatin ( $\geq$ 98% purity), acetic acid, butanoic acid, triphenylphosphine (Ph<sub>3</sub>P), iodine (I<sub>2</sub>), 4-dimethylaminopyridine (DMAP), and all solvents (analytical grade) were purchased from Sigma-Aldrich (USA) and used without further purification. Silica gel plates were employed for thin-layer chromatography (TLC) to monitor reaction progress.

#### Devices and Instruments

instrumentation. Melting points were determined using a Thermo Fisher apparatus (UK) at the Chemistry Department, College of Science, University of Basrah. Thin-layer chromatography (TLC) was performed on Merck silica gel plates (Germany) using ethyl acetate: n-hexane (7:3) as eluent, with spot visualization under

ISSN: **2229-7359** Vol. 11 No. 18s, 2025

https://www.theaspd.com/ijes.php

UV light and iodine vapors. FT-IR spectra were recorded in the range 4000–400 cm<sup>-1</sup> using a BRUKER ALPHA II spectrometer (Germany) at the same department. <sup>1</sup>H and <sup>13</sup>C-NMR spectra were obtained using a Bruker 400 MHz (Advance UltraShield) NMR spectrometer with DMSO-d<sub>6</sub> as solvent and TMS as internal standard at the College of Education, University of Basrah. Mass spectra were recorded using an Agilent Technologies (HP 5973C) EI mass spectrometer at 70 eV ionization energy at the Faculty of Chemistry, Tarbiat Modares University, Tehran, Iran.

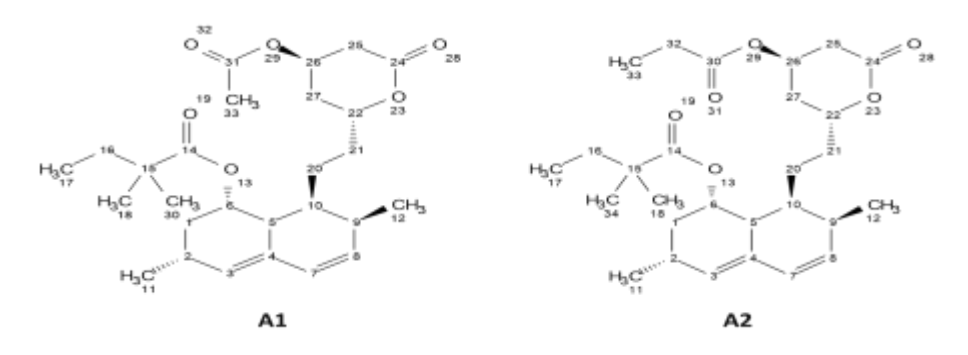
Compounds Synthesis (Sardarian et al., 2009)

Synthesis of simvastatin acetate ester (A1)

In a 25 mL round-bottom flask, triphenylphosphine (Ph<sub>3</sub>P, 0.39 g, 1.5 mmol) and iodine (I<sub>2</sub>, 0.38 g, 1.5 mmol) were dissolved in 5 mL of dry dichloromethane (CH<sub>2</sub>Cl<sub>2</sub>) under ambient conditions. Acetic acid (0.09 gm, 1.5 mmol) and 4-dimethylaminopyridine (DMAP, 0.45 g, 3.7 mmol) were added sequentially to the solution. The reaction mixture was stirred for 5 minutes at room temperature. Subsequently, an alcohol (simvastatin) (0.627 gm, 1.5 mmol) was added dropwise, and the progress of the reaction was monitored by thin-layer chromatography (TLC) using aluminum-backed silica gel plates, scheme 1. Complete consumption of the starting materials was observed within 15 minutes. The crude product was then purified by column chromatography on silica gel using a mixture of ethyl acetate and n-hexane (7:3, v/v) as eluent to form a yellow-brown solid in a 88% yield, M.p. 84-86°C and Rf=0.63. FT-IR (v, cm<sup>-1</sup>): 1246.35m, 1713.8s, 2927.89w, 2878.5w, 720.43s, 1156.06s. Mass spectrum m/z=462.29, 122.7, 173.8, 191.2, 79.1, 401.1, and 43.02. <sup>1</sup>H NMR and <sup>13</sup>C-NMR DMSO-d6 ( $\delta$ , ppm) are shown in Table 1 with figure 2.

Synthesis of simvastatin propionate ester (A2)

In a 25 mL round-bottom flask, triphenylphosphine (Ph<sub>3</sub>P, 0.39 g, 1.5 mmol) and iodine (I<sub>2</sub>, 0.38 g, 1.5 mmol) were dissolved in 5 mL of dry dichloromethane (CH<sub>2</sub>Cl<sub>2</sub>) under ambient conditions. To the resulting solution, propanoic acid (0.111 g, 1.5 mmol) and 4-dimethylaminopyridine (DMAP, 0.45 g, 3.7 mmol) were added sequentially. The reaction mixture was stirred for 5 minutes at room temperature. Subsequently, an alcohol (simvastatin) (0.627 gm, 1.5 mmol) was added dropwise, and the progress of the reaction was monitored by thin-layer chromatography (TLC) using aluminum-backed silica gel plates, scheme 1. Complete consumption of the starting materials was observed within 15 minutes. The crude product was then purified by column chromatography on silica gel using a mixture of ethyl acetate and n-hexane (7:3, v/v) as eluent to form a yellow solid in 80% yield, M.p=82-84, and Rf=0.67 . FT-IR (v, cm<sup>-1</sup>): 1244.87w, 1713.74s, 2930.95w, 2877.93w, 720.36s, 1155.62s. Mass spectrum m/z=476.3, 279.1, 122.7, 44.3. 1H NMR DMSO-d6 ( $\delta$ , ppm) and <sup>13</sup>C-NMR shown in table 1 with figure 2(Rakhmatullin et al., 2016).



Figures 2: Structure of new compounds A1 & A2

ISSN: **2229-7359** Vol. 11 No. 18s, 2025

https://www.theaspd.com/ijes.php

Table 1:1H-NMR and 13C-NMR

comp	¹H-NMR	<sup>13</sup> C-NMR	Co mp	¹H-NMR	<sup>13</sup> C·NMR
A1	1.94-2.05 (m,1H, H-1, ov. with H-28) 2.17-2.35 (m, 1H, H-2) 5.89-5.94 (d, 1H, H-3) 2.23-2.30 (dd, 1H, H-5) 4.76-4.81 (m, 1H, H-6) 5.89-5.94 (d, 1H, H-7) 5.69-5.75 (dd, 1H, H-8) 2.16-2.38 (m, 1H, H-9) 1.59-1.68 (m, 1H, H-10) 1.17-1.28 (d, 3H, H-10) 1.17-1.28 (d, 3H, H-11) 0.77-0.88 (d, 3H, H-12) 0.92-0.93 (d, 3H, H-12) 0.92-0.93 (d, 3H, H-13) 1.47-1.58 (m, 2H, H-16) 1.62-1.72 (t, 3H, H-17) 0.72-0.73 (t, 3H, H-17) 0.72-0.73 (t, 3H, H-18) 1.1 (s, 3H, H-20) 1.32-1.47 (m, 2H, H-21) 4.44-4.48 (m, IH, H-22) 2.61-2.67 (m, 2H, H-25) 5.05-5.12 (m, 2H, H-27) 1.84-1.95 (m,2H, H-28, ov. With H-1)	34.92(C-1) 27.15 (C-2) 131.86 (C-3) 133.68 (C-4) 40.82 (C-5) 78.35 (C-6) 129.18 (C-7) 141.76 (C-8) 30.54 (C-9) 40.69 (C-10) 23.16 (C-11) 14.05 (C-12) 177.02 (C-14) 44.89 (C-15) 31.81 (C-16) 9.62 (C-17) 24.87 (C-18) 24.13 (C-20) 31.81 (C-21) 79.92 (C-22) 172.63 (C-24) 36.58 (C-25) 62.76 (C-26) 35.73 (C-27) 170.69 (C-30) 21.71 (C-32) 24.93 (C-33)	A2	1.91-2.07 (m, 2H, H-1, ov. With H-27) 2.16-2.2.33(m,1H, H-2) 5.85-5.91 (d, 1H, H-3) 2.51 (d, 1H, H-5) 5.01-5.04 (m, 1H, H-6) 5.90-5.92 (m, 1H, H-7) 5.02-5.14 (dd, 1H, H-8) 2.15-2.22 (m, 1H, H-9) 1.54-1.66 (m, 1H, H-10) 1.21-1.25 (d, 3H, H-11, ov. With H-18) 0.75-0.77 (d, 3H, H-12) 1.54-1.66 (m, 1H, H-16) 0.88-0.91 (t, 3H, H-17) 1.14 (s, 3H, H-18, ov. With, H-33) 1.41-1.43 (m,2H, H-20, ov. With H-21) 1.43-1.54 (m, 2H, H-21, ov. With H-20) 4.79-4.83 (m, 1H, H-22) 2.73-2.93 (m, 2H, H-25) 5.14 (m, 1H, H-26) 5.05-5.14 (m, 2H, H-32, ov. With H-2) 1.1-1.2 (m, 3H, H-33) 1.2 (s, 3H, H-34, ov. With H-18)	35.22 (C-1) 29.30 (C-2) 132.35 (C-3) 133.42 (C-4) 41.99 (C-5) 68.28 (C-6) 131.82 (C-7) 140.79 (C-8) 30.50 (C-9) 41.99 (C-10) 23.72 (C-11) 14.05 (C-12) 177.02 (C-14) 45.94 (C-15) 32.89 (C-16) 14.05 (C-17) 27.46 (C-18) 26.98 (C-20) 32.89 (C-21) 80.06 (C-22) 164.23 (C-24) 37.21 (C-25) 77.91 (C-26) 36.57 (C-27) 29.3 (C-32) 9.61 (C-33) 27.46 (C-34)

ISSN: **2229-7359** Vol. 11 No. 18s, 2025

https://www.theaspd.com/ijes.php

Scheme 1: Synthesis of compounds [A1&A2].

# **Experimental Animals**

Adult male albino rats were used in this study to conduct biological evaluations of synthetic compounds derived from simvastatin. These rats were obtained from a specially equipped animal vivarium and allowed to acclimatize for 2 weeks before the experiment. The study included 30 rats weighed between (200 & 250) gm and were housed under controlled environmental conditions, including temperature (22  $\pm$  2 °C), relative humidity (55–65%), and a 12-hour light/dark cycle(Mustafa & Abdulah, 2019)

# Induction of hypercholesterolemia

To induce Hypercholesterolemia in the animals, they were divided into two groups. The first group included 6 rats Normal Control (N.C., not exposed to dietary cholesterol), while the second group included 24 rats (P.C) was induced Hypercholesterolemia in the blood by oral administration of purified cholesterol dissolved in soybean oil for four weeks.. The diet was cholesterol-free, ensuring that dyslipidemia resulted solely from the administered cholesterol. Unlike the dietary induction method used, direct dosing guarantees uniform exposure, eliminating variability caused by differences in individual food intake among the experimental rats(Kasim Suker et al., 2013). The dosage of cholesterol was calculated based on each rat's body weight, and the total dose did not exceed 2 gm/kg of body weight per day to avoid overloading the stomach(Ali et al., 2023a). The animals were monitored throughout the treatment period to monitor their general health, weight changes, and behavior(Verma et al., 2016).

# Blood Sample Collection

After 12 hours of fasting, animals were anesthetized intraperitoneally with Xylazine (5 mg/kg) and Ketamine (50 mg/kg). Blood samples were collected via cardiac puncture using sterile syringes to ensure adequate volume for full biochemical analysis (Ali et al., 2023b). Samples were allowed to clot at room temperature for 30–60 minutes, then centrifuged at 3,000 rpm for 15 minutes to obtain serum. The serum was analyzed immediately without freezing to preserve enzymatic and lipid integrity. All steps were conducted under sterile conditions to maintain sample quality (Abd-Alqader et al., 2023; Varghese et al., 2025).

#### Treatment Protocol

Following the successful induction of hypercholesterolemia, rats were randomly divided into five groups (n = 6 per group): a Normal Control (N.C.), a hypercholesterolemia control (P.C), and three treatment groups

ISSN: **2229-7359** Vol. 11 No. 18s, 2025

https://www.theaspd.com/ijes.php

receiving compounds A1, A2, and simvastatin (SIM). All compounds were freshly dissolved in 10% polyethylene glycol 400 (PEG 400) as a vehicle to enhance solubility and ensure dose uniformity (Di Stasi et al., 2010). Treatments were administered orally via gavage at a dose of 50 mg/kg body weight once daily for 30 consecutive days. The dose was adjusted individually based on each rat's body weight. Control groups received an equivalent volume of carrier (10% PEG) only (T.-W. Kim et al., n.d.). No dietary or caloric restrictions were applied during the study period. At the end of treatment, blood samples were collected via cardiac puncture under sterile conditions to obtain sufficient serum for biochemical analysis (Al-Fartosy Sameerah Ahmed Zearah & Alwan, 2013).

# Biochemical Analysis of Lipid Profile

All biochemical serum analyses, including the lipid profile parameters-total cholesterol (TC), triglycerides (TG), high-density lipoprotein cholesterol (HDL-C), low-density lipoprotein cholesterol (LDL-C), very-low-density lipoprotein cholesterol (VLDL-C), as well as liver function enzymes, alanine aminotransferase (ALT) and aspartate aminotransferase (AST), alkaline Phosphatase (ALP) and bilirubin levels were measured using an automated clinical chemistry analyzer (Cobas c 111, Roche Diagnostics, Germany). All measurements were carried out employing enzymatic colorimetric methods with commercially available kits supplied by Roche.

# Statistical Analysis

All data were expressed as mean ± standard deviation (SD). Statistical analysis was performed using the Statistical Package for the Social Sciences (SPSS) software, version [insert version number]. One-way analysis of variance (ANOVA) followed by Tukey's post hoc test was applied to assess the statistical significance among groups. A p-value less than 0.05 was considered statistically significant.

# **RESULT AND DISCUSSION**

Structural Clarification of Synthesized Compounds (A1 and A2)

The synthesized ester derivatives of simvastatin (A1 and A2) were characterized using a combination of FT-IR, <sup>1</sup>H-NMR, <sup>13</sup>C-NMR, and mass spectrometry to confirm their molecular structures and functional group modifications.

#### FT-IR Spectroscopy

Figures 3 and 4 show that the Fourier transform infrared (FT-IR) spectra of compounds A1 and A2 exhibited distinct absorption bands, confirming the successful esterification process. In both derivatives, strong bands appeared at approximately 1713cm<sup>-1</sup>, corresponding to the esterified carbonyl (C=O) stretching vibration(Sardarian et al., 2009), which was absent in the spectrum of the original simvastatin. In addition, a marked shift in the hydroxyl band was observed: the broad O-H stretch of simvastatin (approximately 3550–3450 cm<sup>-1</sup>) significantly disappeared, confirming the formation of an ester at the hydroxyl site(Bonthagarala et al., 2013). We also observed C-H stretching vibrations of the methyl and methylene groups at approximately 2920–2960 cm<sup>-1</sup>, while C-O-C stretches appeared at approximately 1170–1200 cm<sup>-1</sup>. Together, these spectral changes provide evidence for the formation of an ester linkage in both A1 (acetate) and A2 (propanoate) derivatives.

ISSN: **2229-7359** Vol. 11 No. 18s, 2025

https://www.theaspd.com/ijes.php

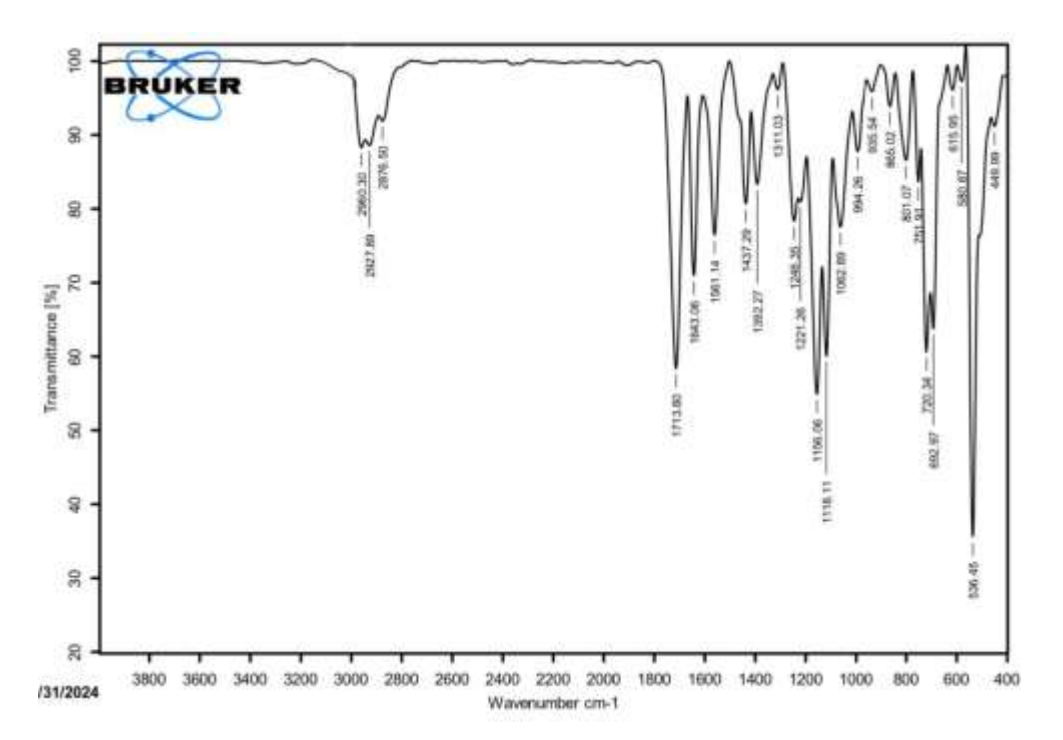


Figure 3: FT-IR spectrum of compound A1

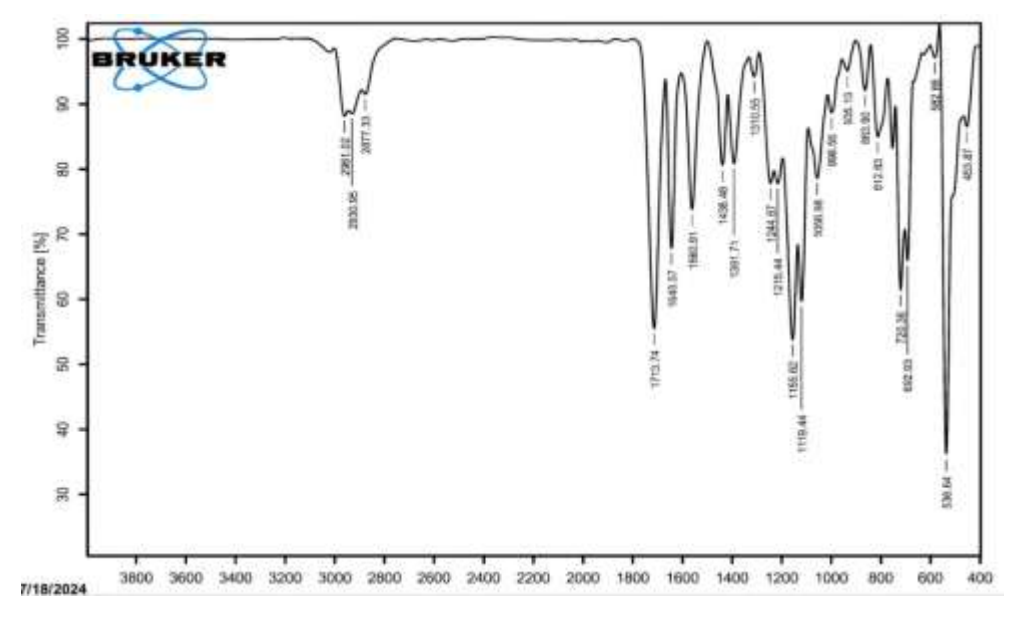


Figure 4: FT-IR spectrum of compoundA2

# <sup>1</sup>H-NMR Spectroscopy

Figures 5 and 6 show the H NMR spectra of compounds A1 and A2 (recorded in DMSO<sub>6</sub>). The chemical shifts and integration values were consistent with the proton environments predicted in the esterified structures. The methyl protons of the acetate group (A1) appeared as a single group at  $\delta$  ~2.08 ppm, confirming successful acetylation. In A1, the butanoate chain exhibited triplet and multiplet signals in the aliphatic region between  $\delta$  0.88–2.30 ppm, attributed to the terminal methyl and methylene groups. In both

ISSN: **2229-7359** Vol. 11 No. 18s, 2025

https://www.theaspd.com/ijes.php

compounds, the characteristic signals of the decalin ring and the lactone molecule of simvastatin remained intact, indicating that esterification occurred selectively at the hydroxyl group of the side chain without disrupting the primary structure(Rakhmatullin et al., 2016).

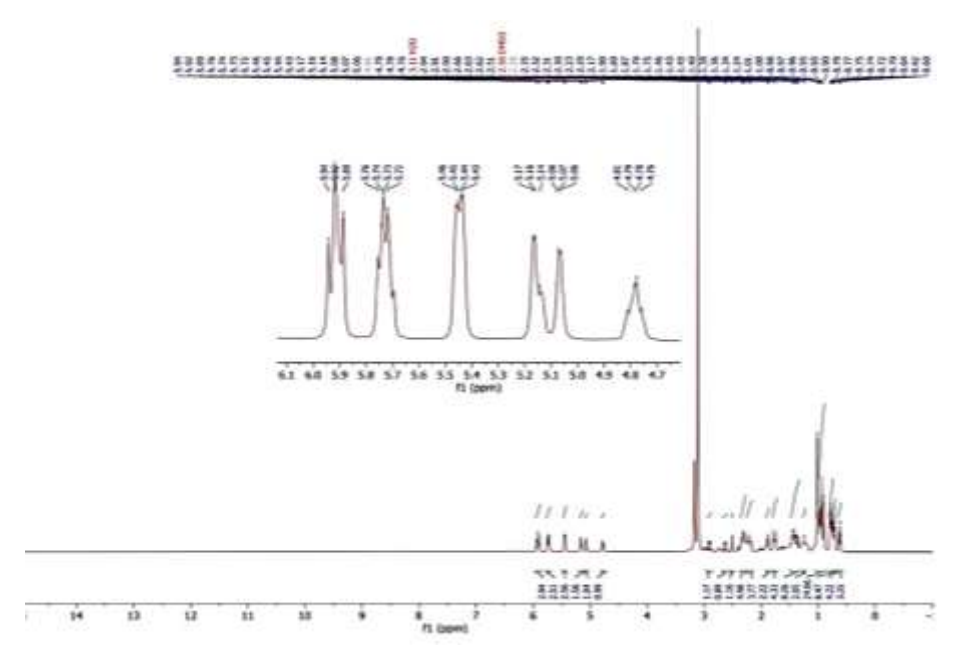


Figure 5:1H-NMR Spectrum of Compound A1

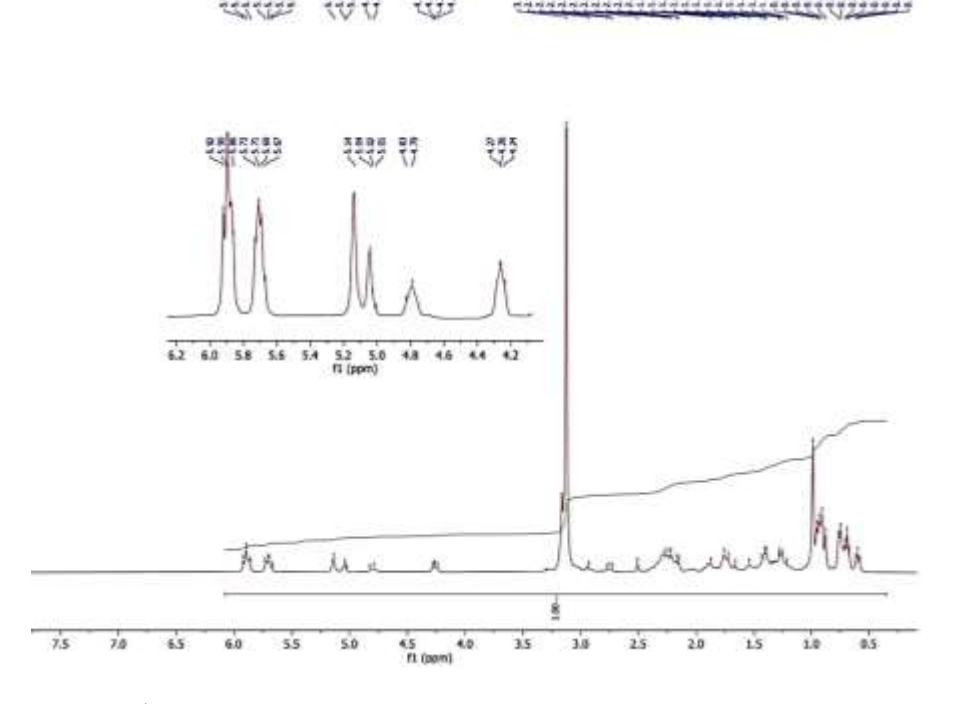


Figure 6: <sup>1</sup>H-NMR Spectrum of Compound A2

<sup>&</sup>lt;sup>13</sup>C-NMR Spectroscopy

ISSN: **2229-7359** Vol. 11 No. 18s, 2025

https://www.theaspd.com/ijes.php

Figures 7and 8 show the  $^{13}$ C-NMR spectra further confirmed structural integrity and ester formation. A1 showed a distinct ester carbonyl carbon signal at  $\delta$   $^{\sim}$ 170–172 ppm. The acetate methyl carbon appeared at  $^{\sim}$ 21 ppm. Additional aliphatic carbon signals related to the prpanoate chain in compound (A2) were evident, with the ester carbonyl around  $\delta$   $^{\sim}$ 173 ppm and aliphatic carbons between  $\delta$  13–35 ppm. The consistent presence of characteristic carbon signals of the simvastatin backbone (e.g.,  $\delta$   $^{\sim}$ 74–80 ppm for C–O carbons, and  $\delta$   $^{\sim}$ 35–50 ppm for methylene bridges) supports the successful modification while retaining the original scaffold(Andrews, 2015).

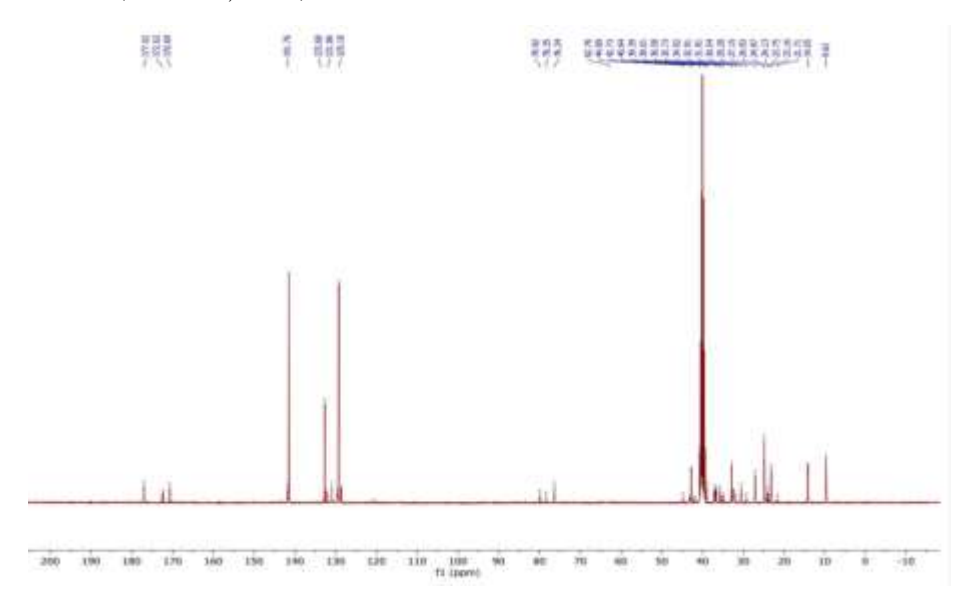


Figure 7: <sup>13</sup>C-NMR Spectrum of compound A1

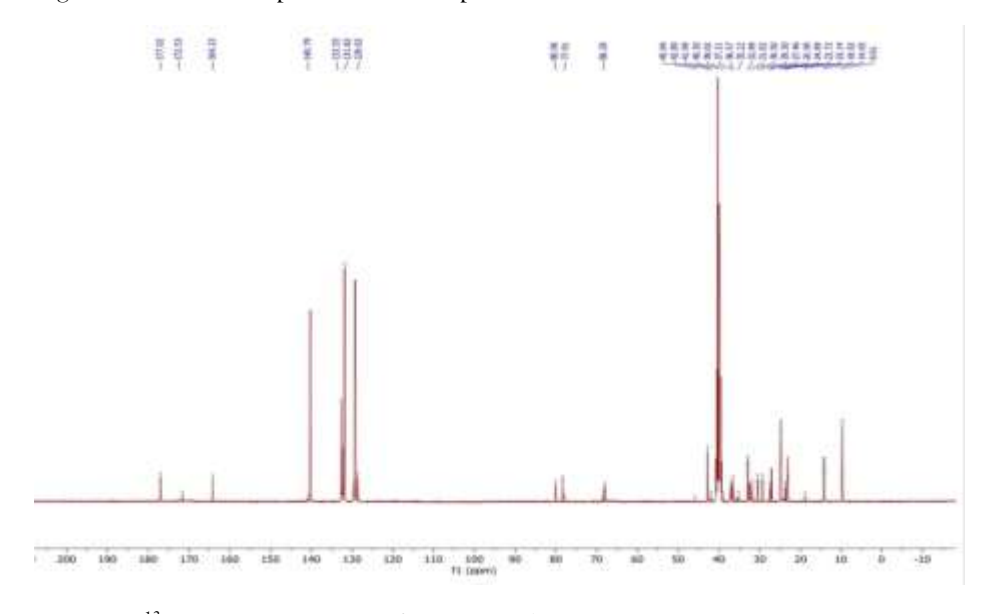


Figure 8: <sup>13</sup>C-NMR Spectrum of compound A2

Mass Spectrometry

ISSN: **2229-7359** Vol. 11 No. 18s, 2025

https://www.theaspd.com/ijes.php

Figures 9&10 the mass spectra of A1 and A2 confirmed their molecular weights and fragmentation patterns. Compound A1 exhibited a molecular ion peak  $[M^+]$  at m/z = 462.29, while A2 displayed  $[M^+]$  at m/z = 476.3. Aligning with their calculated molecular weights, both compounds showed a base peak at m/z = 122.7, indicative of a common fragment ion derived from the simvastatin core structure after side-chain cleavage. Other key fragments appeared at m/z = 291, 401.1,279.1, consistent with loss of ester groups and sequential cleavage of the aliphatic chain(Tete et al., 2020; Wong, 2015).

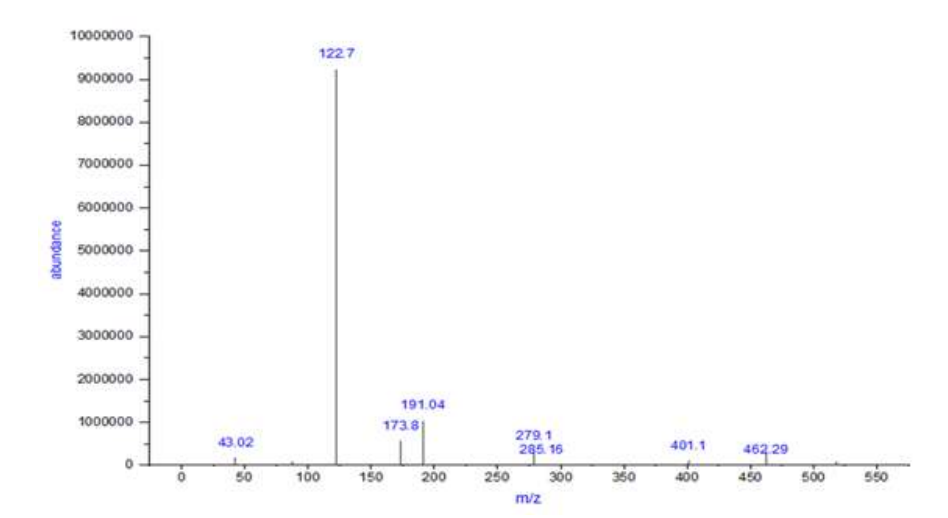


Figure 9: mass spectrum of compounds A1

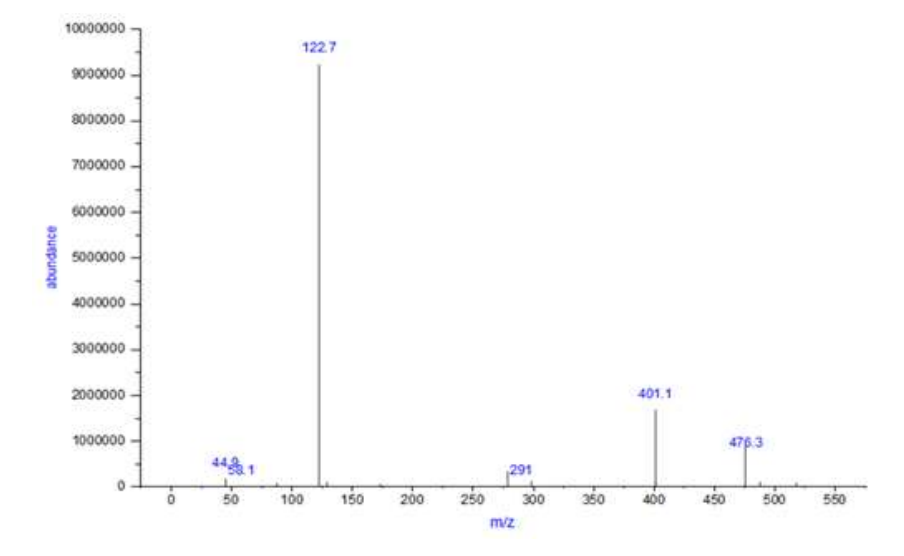


Figure 10: mass spectrum of compounds A2

Hyperlipidemia induction protocol

effect of cholesterol-induction on lipid profile (induction phase)

Hyperlipidemia was experimentally induced in healthy albino rats via oral administration of purified cholesterol dissolved in soybean oil at a concentration of 2 g/kg body weight, delivered daily for 30

ISSN: **2229-7359** Vol. 11 No. 18s, 2025

https://www.theaspd.com/ijes.php

consecutive days. This pharmacological induction approach, rather than dietary modification, enabled a rapid and reproducible elevation in serum lipid levels, effectively mimicking the biochemical hallmarks of human dyslipidemia. As shown in Table 2, the (P.C) exhibited statistically significant elevations (p < 0.0001) in all atherogenic lipid parameters compared to the untreated normal control (N.C). Serum total cholesterol (TC) increased markedly from  $51.68 \pm 7.75$  mg/dL in the N.C to  $87.11 \pm 8.98$  mg/dL in P.C. Likewise, triglycerides (TG) rose from  $26.10 \pm 5.21$  to  $54.66 \pm 6.25$  mg/dL; low-density lipoprotein cholesterol (LDL-C) increased from  $17.68 \pm 5.13$  to  $42.67 \pm 3.62$  mg/dL; and very low-density lipoprotein cholesterol (VLDL-C) levels doubled from  $5.22 \pm 1.07$  to  $10.60 \pm 1.09$  mg/dL. (Chen et al., 2022; Y. J. Kim et al., 2023; Rahmat Ullah et al., 2023; Wang et al., 2021)

Interestingly, high-density lipoprotein cholesterol (HDL-C), typically considered a protective marker, exhibited a inconsistent yet significant decline from 31.40 ± 7.19 to 26.59 ± 7.29 mg/dL in the P.C. This reduction likely reflects a dysregulation of reverse cholesterol transport (RCT) mechanisms and impaired hepatic lipid homeostasis, contributing to the improvement of an atherogenic lipid profile. These observations collectively confirm the successful establishment of a chemically induced hypercholesterolemic state that is marked by elevated TC, LDL-C, VLDL-C, and TG, alongside reduced HDL-C. The pathological condition produced closely mirrors early-stage human hyperlipidemia, thus providing a robust and reliable preclinical model(Ouimet et al., 2019).

This model served as a consistent platform to evaluate the lipid-lowering potential of newly synthesized simvastatin derivatives (A1 and A2), in comparison to the standard reference drug simvastatin. The reproducibility and specificity of this induction approach further underscore its value in pharmacological screening of therapeutic agents targeting cholesterol biosynthesis, lipoprotein metabolism, and lipid transport mechanisms..

Table 2: Comparison of Lipid Profile parameters between normal control and cholesterol-Induced Group (Induction Phase)

Groups(n=6)	Parameters (mean ±SD)					
	T.C	TG	LDL-C	HDLC	VLDL-C	
N.C	51.68±7.75	26.10±5.21	17.68±5.13	31.40±7.19	5.22±1.07	
P.C	87.11±8.98	54.66±6.25	42.67±3.62	26.59±7.29	10.60±1.09	
P-value	0.0001	0.0001	0.0001	0.0012	0.0001	

Data are expressed as mean ± standard deviation (SD). Statistical analysis was performed using independent sample t-test. A p-value less than 0.05 was considered statistically significant.

Histological Evaluation During the Induction Phase

Histological observations reinforced the biochemical findings. The P.C exhibited classic features of nephrotoxicity, including glomerular atrophy, tubular epithelial cell desquamation, and interstitial inflammation, figures 11 and 12, in agreement with literature on cholesterol-induced glomerulosclerosis and tubular damage. These changes reflect lipid accumulation in renal parenchyma, altered vascular integrity, and cytokine-driven cellular injury. In contrast, The normal control group, maintained a well-preserved renal architecture with intact glomeruli, narrow Bowman's space, and organized tubules (Figure 11), validating the healthy baseline (Hasan et al., 2024; Mazzali et al., 2001).

ISSN: **2229-7359** Vol. 11 No. 18s, 2025

https://www.theaspd.com/ijes.php

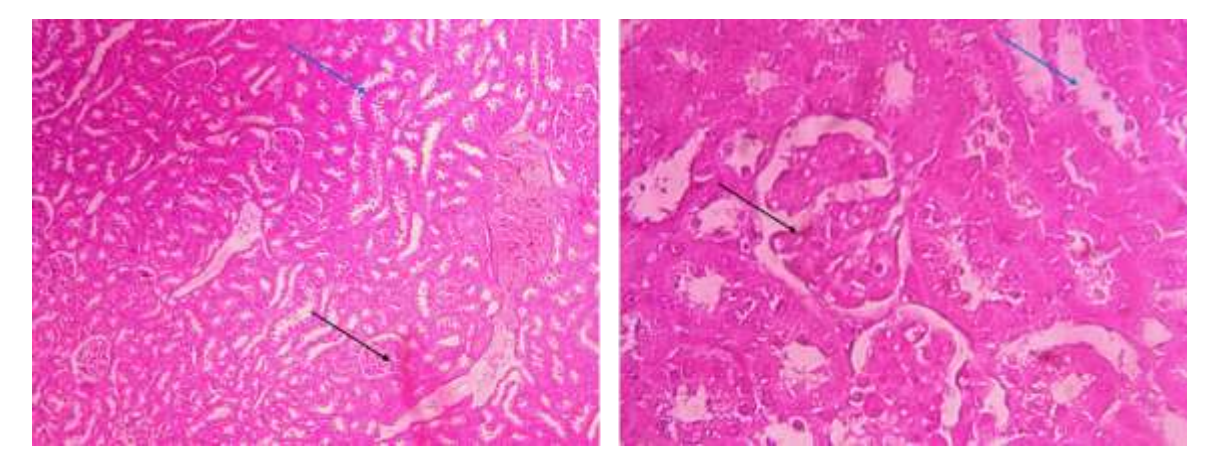


Figure 11: The kidney section from the N.C group displays preserved renal cortical architecture with clearly delineated glomeruli (black arrow), intact Bowman's spaces (blue arrow), and uniform tubular epithelial lining. No signs of inflammation, necrosis, or cellular degeneration are observed. H&E stain, 10X & 40X.

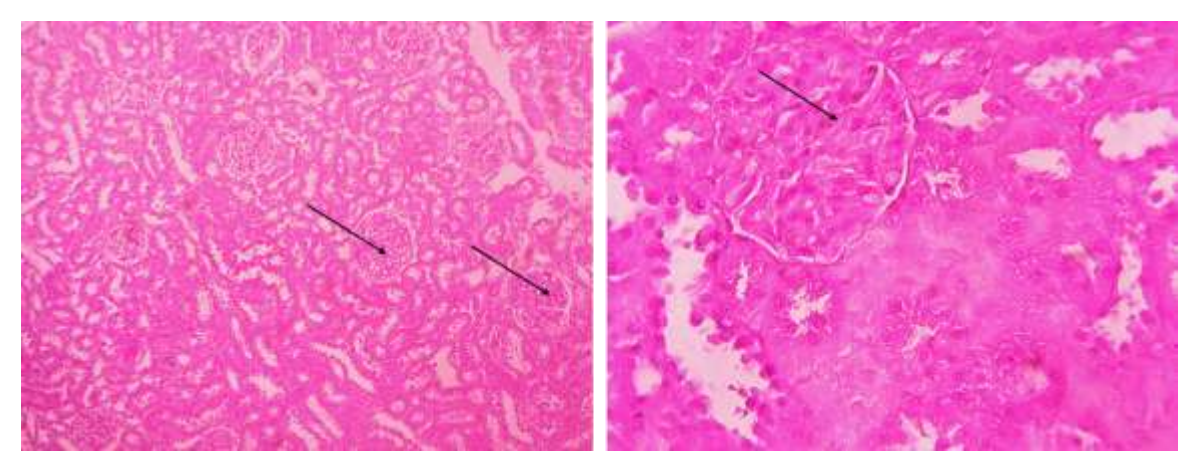


Figure 12: The P.C group shows distinct histopathological alterations characterized by glomerular shrinkage and atrophy, widened Bowman's spaces (blue arrows), and evidence of tubular epithelial cell desquamation (red arrows). Focal tubular necrosis and interstitial inflammation are evident, indicating cholesterol-induced nephrotoxicity. H&E stain, 10X & 40X.

Effect of Treatments on kidney Function Biomarkers in Cholesterol-Induced Rats

Serum Biomarker Analysis (Urea and Creatinine)

The data summarized in Table 3 demonstrate the alterations in serum levels of urea and creatinine among experimental groups subjected to cholesterol-induced hyperlipidemia and subsequent treatment with simvastatin and its synthesized analogues (A1 and A2). Administration of 2 g/kg cholesterol for 30 consecutive days led to a significant increase in serum urea and creatinine in the hyperlipidemic control group (P.C), with values reaching  $64.45 \pm 3.19$  mg/dL and  $0.37 \pm 0.04$  mg/dL, respectively. This elevation indicates an apparent impairment of renal function associated with the accumulation of metabolic waste products, most likely due to lipid-induced renal oxidative stress and glomerular injury, as previously described in similar rat models (da Silva et al., 2024). Compared to the P.C group, rats treated with Simvastatin and its A2 derivative showed a statistically significant reduction in serum urea levels (30.92  $\pm$  4.19 and 29.62  $\pm$  6.08 mg/dL, respectively; p < 0.001), indicating a marked nephroprotective effect. This reduction is likely mediated

ISSN: **2229-7359** Vol. 11 No. 18s, 2025

https://www.theaspd.com/ijes.php

through improved endothelial function, decreased oxidative burden, and downregulation of proinflammatory mediators, consistent with the pleiotropic actions of statins and their analogues. However, creatinine levels in these two groups  $(0.33 \pm 0.03)$  for SIM and  $0.36 \pm 0.04$  mg/dL for A2) remained statistically non-significant compared to P.C (p = 0.098), suggesting a milder improvement in glomerular filtration rate. Of particular interest is compound A1, which produced the most pronounced reduction in serum urea (15.75  $\pm$  2.55 mg/dL), achieving a highly significant difference versus P.C (p < 0.001). This effect was also distinct from N.C (p < 0.01), suggesting that A1 may exert superior diuretic or detoxification enhancement, potentially linked to its unique side chain structure (Najafi et al., 2023). Interestingly, although creatinine levels in A3-treated rats (0.34 ± 0.08 mg/dL) were moderately improved, the change did not reach statistical significance when compared with P.C, highlighting that urea may be a more sensitive early marker of functional improvement in this model. In contrast, the normal control group (N.C) maintained stable urea  $(33.14 \pm 3.77 \text{ mg/dL})$  and creatinine  $(0.27 \pm 0.04 \text{ mg/dL})$  levels throughout the experimental period, confirming the physiological baseline for comparison. The significant disparity in urea values across the groups (p  $\leq$  0.001) underscores the efficacy of both native and modified statins in reversing lipid-induced nephrotoxicity. Taken together, these findings highlight the potential of the synthesized analogues, particularly Al and A2, to ameliorate kidney function disturbances induced by hyperlipidemic conditions, and warrant further mechanistic and histopathological investigations

Table 3: Effect of Simvastatin-Derived Compounds and Simvastatin on Kidney Function Markers in Hypercholesterolemic Rats

Groups	Parameters (mean ±SD)			
No.6	Urea (mg/dl)	Creatinine (mg/dl)		
N.C	33.14±3.77B	0.27±0.04D		
P.C	64.45±3.19A	0.37±0.04A		
A1	15.75±2.55C	0.34±0.08A		
A2	29.62±6.08B	0.36±0.04B		
SIM	30.92±4.19B	0.33±0.03BC		
P-value	<0.001	<0.001		

Values expressed in letters (A, B, and C) within a row represent mean significant differences at the p < 0.05 level among the groups. The different letters between the groups represent significant differences (p < 0.05).

ISSN: **2229-7359** Vol. 11 No. 18s, 2025

https://www.theaspd.com/ijes.php

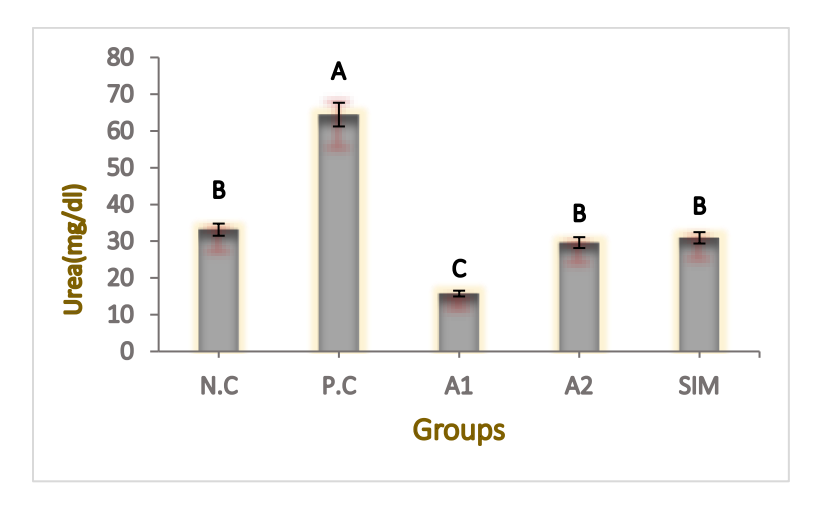


Figure 11: The serum concentrations of Urea in treated groups with A1, A2, SIM compared to normal (N.C) and hyperlipidemic control (P.C) groups.

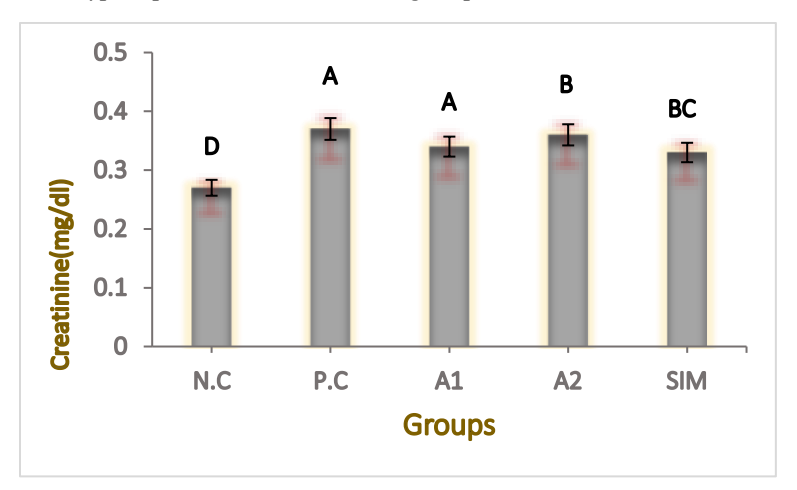


Figure 12: The serum concentrations of Creatinine in treated groups with A1, A2, SIM compared to normal (N.C) and hyperlipidemic control (P.C) groups.

Histopathological Evaluation of Aland A2 Treatments

Histological examination of renal tissues reinforced the biochemical findings and revealed variable degrees of structural renal recovery among the treatment groups (Figures 13-16). The cholesterol-fed control group (P.C) showed pronounced glomerular degeneration, tubular dilation, and widespread interstitial inflammation, confirming cholesterol-induced nephrotoxicity(Eldesoqui et al., 2024; Ren et al., 2023). Notably, rats treated with compound A1 exhibited the most pronounced histological recovery among all treatment groups. The glomeruli were clearly restructured with restored architecture, and the renal tubules appeared largely intact, showing minimal swelling or vacuolar changes. Inflammatory cell infiltration was significantly reduced compared to the P.C group, and nephron alignment was visibly improved. These morphological improvements are consistent with the marked reduction in serum urea observed in this group, indicating a strong renoprotective effect possibly mediated by structural modifications that enhance anti-inflammatory and antioxidant activities(Cattaneo & Remuzzi, 2005). In comparison, the A2-treated group displayed a moderate degree of histological improvement. While glomeruli were partially preserved and some tubular organization was evident, signs of tubular irregularity and residual inflammatory infiltration remained.

ISSN: **2229-7359** Vol. 11 No. 18s, 2025

https://www.theaspd.com/ijes.php

Tubular dilation was more noticeable than in the A1, suggesting that A2 provided limited yet meaningful renal protection, in alignment with the partial biochemical improvement in urea and creatinine levels. The SIM-treated group, which received native simvastatin, demonstrated intermediate outcomes. Histological sections revealed partially preserved glomeruli and mild tubular regeneration; however, focal regions showed persistent tubular dilation and interstitial infiltration(Preta, 2022). These findings suggest a moderate nonprotective effect, though less effective than A1 and comparable to A2, which correlates with its intermediate serum biomarker levels. The histopathological findings affirm the superior nephroprotective profile of compound A1 over A2 and simvastatin. The data further support the hypothesis that structural modification of statins may enhance their therapeutic potential against cholesterol-induced renal injury.

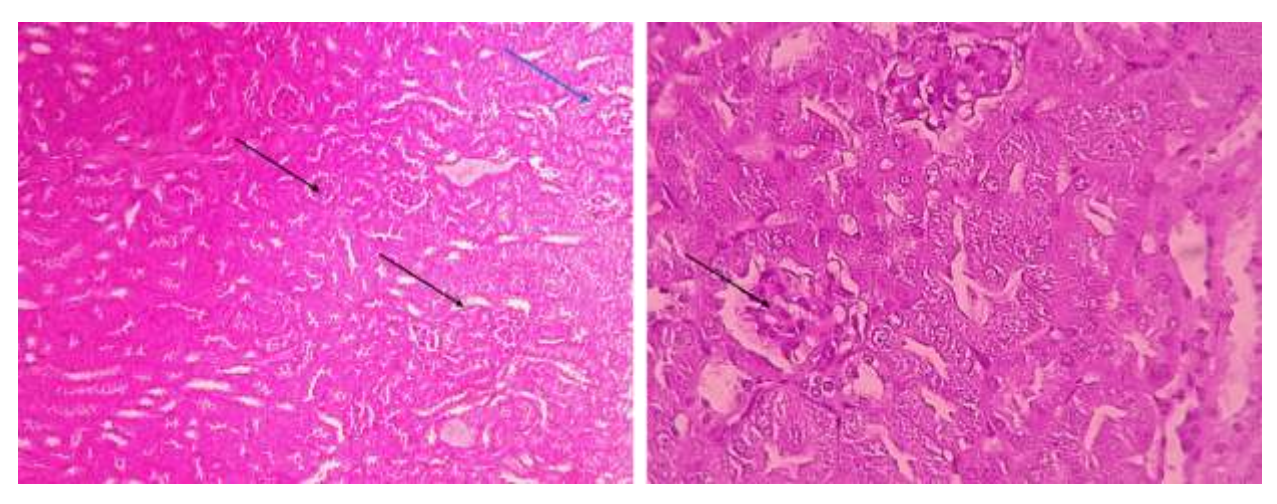


Figure 13: Sections from the P.C show disrupted renal architecture with degenerated glomeruli (black arrow), tubular dilation (red arrow), and marked inflammatory infiltration (blue arrow). These findings indicate cholesterol-induced nephrotoxicity. H&E stain, 4X & 10X

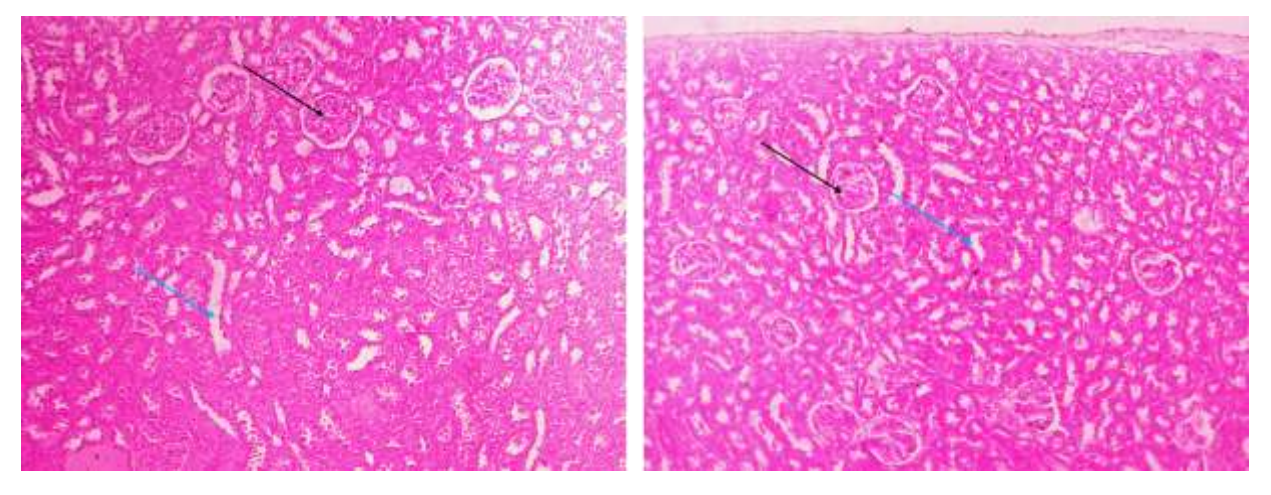


Figure 14: Kidney sections from A1-treated animals show partially restored glomeruli (black arrow) with some tubular swelling and persistent interstitial infiltration (blue arrow), indicating moderate protection with residual injury. H&E stain, 4X & 10X

ISSN: **2229-7359** Vol. 11 No. 18s, 2025

https://www.theaspd.com/ijes.php

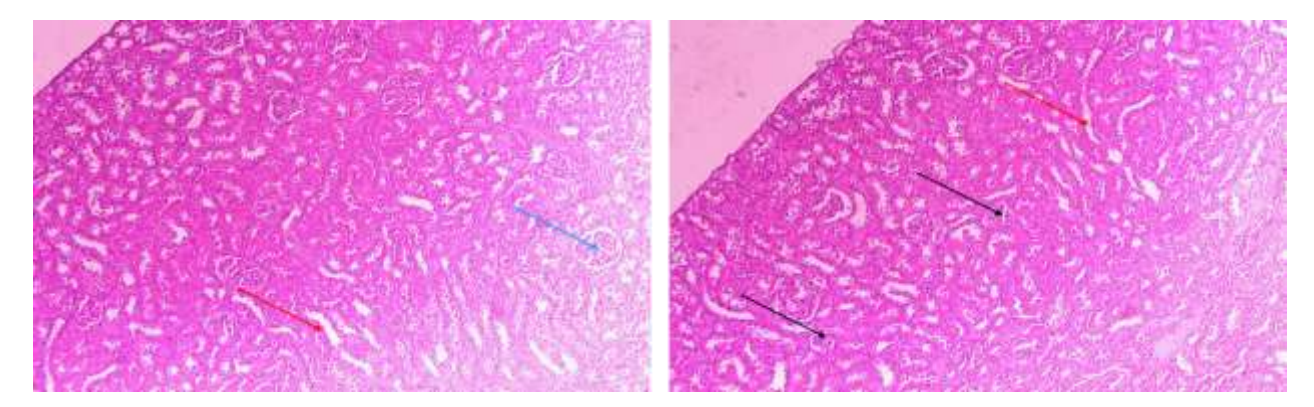


Figure 15: Renal histology from the A2 group shows mild glomerular improvement (black arrow), with tubular irregularities (red arrow) and evident interstitial inflammation (blue arrow), reflecting limited renoprotective effect. H&E stain, 4X & 10X.

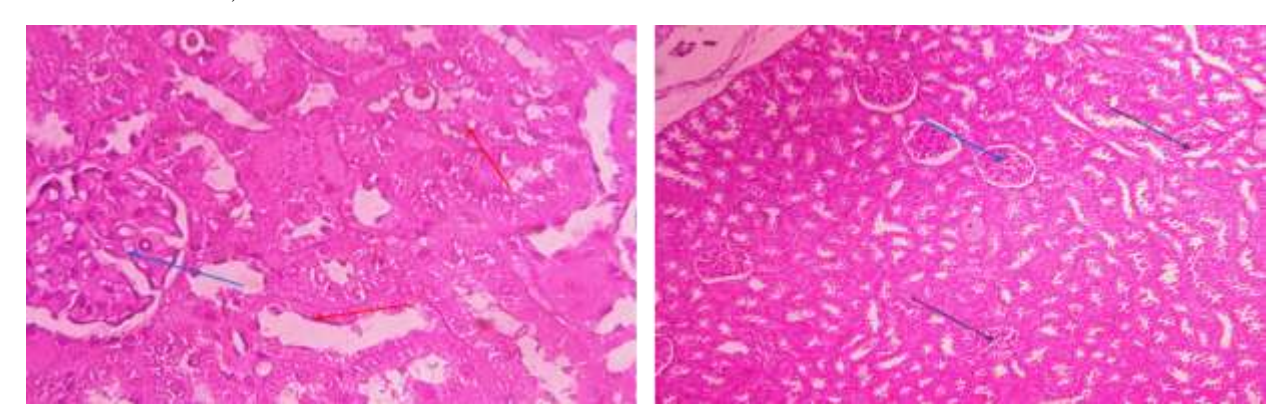


Figure 16: Kidney tissue from the SIM group shows improved glomerular appearance (black arrow), but tubular dilation remains (red arrow), along with mild inflammatory infiltration (blue arrow), suggesting partial renal recovery. H&E stain, 4X & 10X.

#### CONCLUSION

The present study demonstrated that cholesterol-induced hyperlipidemia in rats resulted in significant renal dysfunction, as evidenced by elevated serum urea and creatinine levels and pronounced histopathological alterations. Treatment with simvastatin and its structurally modified analogues (A1 and A2) conferred varying degrees of nephroprotection. Among the tested compounds, A1 exhibited the most substantial renoprotective effect, as reflected by its ability to restore near-normal serum biomarker levels and markedly improve renal histoarchitecture. A2 also displayed moderate protective effects, surpassing those of native simvastatin in some structural aspects, yet falling short of the efficacy observed with A1. These findings suggest that rational chemical modification of the simvastatin scaffold can yield novel analogues with enhanced therapeutic potential against cholesterol-induced renal injury. Further studies are warranted to elucidate the precise molecular mechanisms underlying these protective effects and to evaluate their long-term safety and efficacy in broader biological models

## **REFERENCES**

ISSN: **2229-7359** Vol. 11 No. 18s, 2025

https://www.theaspd.com/ijes.php

 Abd-Alqader, S. M., Zearah, S. A., & Al-Assadi, I. J. (2023). Effect of Curcumin (Standard and Supplement) with Zinc on Reproductive Hormones in Polycystic Ovary Syndrome (PCOS) Rats. Tropical Journal of Natural Product Research, 7(3), 2540–2546. https://doi.org/10.26538/tjnpr/v7i3.12

- 2. Abd-Elghany, A. E., Helmy, O., El-Garhy, M., & Abdelkader, H. (2023). Critical Appraisal of Physiochemical Characteristics of Statins and Drug Delivery Systems for Improving Their Bioavailability. In J. Adv. Biomed. & Pharm. Sci (Vol. 6). http://jabps.journals.ekb.eg
- 3. Al-Fartosy Sameerah Ahmed Zearah, A. J., & Alwan, N. A. (2013). TOTAL ANTIOXIDANT CAPACITY AND ANTIHYPERLIPIDEMIC ACTIVITY OF ALKALOID EXTRACT FROM AERIAL PART OF ANETHUM GRAVEOLENS L. PLANT. In European Scientific Journal (Vol. 9, Issue 33).
- 4. Ali, R. S., Hameed, B., & Shari, F. (2023a). Synergistic antihyperlipidemic effect of alpha lipoic acid with rosuvastatin in high-fat diet-induced hyperlipidemic rats. Romanian Journal of Diabetes, Nutrition and Metabolic Diseases, 30(3), 298–305. https://doi.org/10.46389/rjd-2023-1347
- Ali, R. S., Hameed, B., & Shari, F. (2023b). Synergistic antihyperlipidemic effect of alpha lipoic acid with rosuvastatin in high-fat diet-induced hyperlipidemic rats. Romanian Journal of Diabetes, Nutrition and Metabolic Diseases, 30(3), 298–305. https://doi.org/10.46389/rjd-2023-1347
- 6. Andrews, D. L. (2015). Laser Spectroscopy 1: Basic Principles & Laser Spectroscopy 2: Experimental Techniques (5th edition). Contemporary Physics, 56, 487–488. https://api.semanticscholar.org/CorpusID:119527033
- 7. Bonthagarala, B., Kumar, P., Nama. Dr, S., Khalilullah, S., & Babu, S. (2013). Formulation and evaluation of extended release mucoadhesive microspheres of simvastatin. https://doi.org/10.13140/2.1.2898.7689
- 8. Cattaneo, D., & Remuzzi, G. (2005). Lipid oxidative stress and the anti-inflammatory properties of statins and ACE inhibitors. Journal of Renal Nutrition: The Official Journal of the Council on Renal Nutrition of the National Kidney Foundation, 15 1, 71–76. https://api.semanticscholar.org/CorpusID:23761683
- 9. Chen, L., Li, R., Wang, Z., Zhang, Z., Wang, J., Qiao, Y., Huang, Y., & Liu, W. (2022). Lactate-utilizing bacteria ameliorates DSS-induced colitis in mice. Life Sciences, 288, 120179. https://doi.org/10.1016/j.lfs.2021.120179
- da Silva, I. O., de Menezes, N. K., Jacobina, H. D., Parra, A. C., Souza, F. L., Castro, L. C., Roelofs, J., Tammaro, A., Gomes, S. A., Sanches, T. R., & Andrade, L. (2024). Obesity aggravates acute kidney injury resulting from ischemia and reperfusion in mice. Scientific Reports, 14(1). https://doi.org/10.1038/s41598-024-60365-3
- 11. Di Stasi, S., MacLeod, T., Winters, J., & Binder-Macleod, S. (2010). Effects of Statins on Skeletal Muscle: A Perspective for Physical Therapists. Physical Therapy, 90, 1530–1542. https://doi.org/10.2522/ptj.20090251
- 12. Eldesoqui, M., Mohamed, A. S., Nasr, A. N. A., Ali, S. K., Eldaly, M. M., Embaby, E. M., Ahmed, H. S., Saeed, Z. M., Mohammed, Z. A., & Soliman, R. H. M. (2024). The Renoprotective Effect of Atorvastatin in a Rat Model of High-Fat High-Fructose Diet-Induced Renal Injury. Egyptian Academic Journal of Biological Sciences, D. Histology & Histochemistry, 16(1), 179–194. https://doi.org/10.21608/eajbsd.2024.360842
- 13. Fernandes, G. F. S., Prokopczyk, I. M., Chin, C. M., & Santos, J. L. Dos. (2020). The Progress of Prodrugs in Drug Solubility. https://api.semanticscholar.org/CorpusID:219443276
- 14. Hasan, I. H., Shaheen, S. Y., Alhusaini, A. M., & Mahmoud, A. M. (2024). Simvastatin mitigates diabetic nephropathy by upregulating farnesoid X receptor and Nrf2/HO-1 signaling and attenuating oxidative stress and inflammation in rats. Life Sciences, 340, 122445.
- 15. Kasim Suker, D., Jameel Thamer, S., Jasim, T., & Taha, A. (2013). The effect of maternal diet prior and during pregnancy in rats on obesity development in offspring. In Pelagia Research Library European Journal of Experimental Biology (Vol. 3, Issue 1). www.pelagiaresearchlibrary.com
- Kim, T.-W., Kim, T.-K., Park, H.-J., Lee, M.-J., Park, S.-J., Jo, L., Lee, Y.-H., Kim, Y.-S., & Ahn, B. (n.d.). Comparative Analyses of the Influences of Vehicles on Selected Biological Parameters Following Single-Dose Oral Administration in Sprague-Dawley Rats. International Journal of Toxicology, 0(0), 10915818251330516. https://doi.org/10.1177/10915818251330516
- 17. Kim, Y. J., Nitin, N., & Kim, K. B. (2023). Negligible Toxicokinetic Differences of Glyphosate by Different Vehicles in Rats. Toxics, 11(1). https://doi.org/10.3390/toxics11010067
- 18. Mazzali, M., Hughes, J., Kim, Y.-G., Jefferson, J. A., Kang, D.-H., Gordon, K. L., Lan, H. Y., Kivlighn, S., & Johnson, R. J. (2001). Elevated uric acid increases blood pressure in the rat by a novel crystal-independent mechanism. Hypertension, 38(5), 1101–1106.

ISSN: **2229-7359** Vol. 11 No. 18s, 2025

https://www.theaspd.com/ijes.php

19. Mustafa, T., & Abdulah, H. (2019). Histological Alterations Induced by Atorvastatin Therapeutic Doses in some Organs of Male Albino Rats. Polytechnic Journal, 9(1), 13–16. https://doi.org/10.25156/ptj.v9n1y2019.pp13-16

- 20. Najafi, S., Moshtaghie, A. A., Hassanzadeh, F., Nayeri, H., & Jafari, E. (2023). Design, synthesis, and biological evaluation of novel atorvastatin derivatives. Journal of Molecular Structure. https://api.semanticscholar.org/CorpusID:257215196
- 21. Ouimet, M., Barrett, T. J., & Fisher, E. A. (2019). HDL and Reverse Cholesterol Transport. Circulation Research. https://api.semanticscholar.org/CorpusID:149444907
- 22. Preta, G. (2022). Role of Lactone and Acid Forms in the Pleiotropic Effects of Statins. In Pharmaceutics (Vol. 14, Issue 9). MDPI. https://doi.org/10.3390/pharmaceutics14091899
- 23. Rahmat Ullah, M., Sharifuzzaman Shohan, F. M., Aditi Baroi, J., Bhowmik, P., Abdullah Hil Baky Rupak, M., Abu Bakar Siddiq, M., Islam Pranto, T., Shahjalalur Rahman Siam, M., & Tashin, R. (2023). Article no.AJRCD.110292 Original Research Article Shohan et al. In Asian Journal of Research in Cardiovascular Diseases (Vol. 5, Issue 1). https://www.sdiarticle5.com/review-history/110292
- 24. Rakhmatullin, I. Z., Galiullina, L. F., Klochkova, E. A., Latfullin, I. A., Aganov, A. V., & Klochkov, V. V. (2016). Structural studies of pravastatin and simvastatin and their complexes with SDS micelles by NMR spectroscopy. Journal of Molecular Structure, 1105, 25–29. https://doi.org/10.1016/j.molstruc.2015.10.059
- 25. Ren, L., Cui, H., Wang, Y., Ju, F., Cai, Y., Gang, X., & Wang, G. (2023). The role of lipotoxicity in kidney disease: From molecular mechanisms to therapeutic prospects. Biomedicine & Pharmacotherapy = Biomedecine & Pharmacotherapie, 161, 114465. https://api.semanticscholar.org/CorpusID:257345173
- 26. Sabah Al-Obaidi, N., Hammoodi, O. G., Najem Abd, A., & Salam Al-Mahdawi, A. (n.d.). Benzyl Acetate: A Review on Synthetic Methods. https://www.researchgate.net/publication/362832882
- 27. Sadowska, A., Osiński, P., Roztocka, A., Kaczmarz-Chojnacka, K., Zapora, E., Sawicka, D., & Car, H. (2024). Statins—From Fungi to Pharmacy. In International Journal of Molecular Sciences (Vol. 25, Issue 1). Multidisciplinary Digital Publishing Institute (MDPI). https://doi.org/10.3390/ijms25010466
- 28. Safapoor, S., Yazdani, H., & Shahabi, P. (n.d.). A Review on Synthesis and Applications of Statin Family Drugs as a New Generations of Anti-Blood Medicines. J. Chem. Rev, 2(1), 1–27.
- 29. Sardarian, A., Sardarian, A. R., Zandi, M., & Motevally, S. (2009). One-Pot Synthesis of Carboxylic Acid Esters in Neutral and Mild Conditions by Triphenylphosphine Dihalide [Ph One-Pot Synthesis of Carboxylic Acid Esters in Neutral and Mild Conditions by Triphenylphosphine Dihalide [Ph 3 PX 2 (X=Br, I)]]. In Acta Chim. Slov (Vol. 56). https://www.researchgate.net/publication/228506505
- 30. Su, X., Zhang, L., Lv, J., Wang, J., Hou, W., Xie, X., & Zhang, H. (2016). Effect of statins on kidney disease outcomes: A systematic review and meta-analysis. American Journal of Kidney Diseases, 67(6), 881–892. https://doi.org/10.1053/j.ajkd.2016.01.016
- 31. Tete, V. S., Nyoni, H., Mamba, B. B., & Msagati, T. A. M. (2020). Occurrence and spatial distribution of statins, fibrates and their metabolites in aquatic environments. Arabian Journal of Chemistry, 13(2), 4358–4373. https://doi.org/10.1016/j.arabjc.2019.08.003
- 32. Varghese, R., Anoop, S., K. Venugopal, S., Sooryadas, S., Vasudevan, V. N., P. Panicker, V., S. Nair, S., Jennes, D., & John Martin, K. D. (2025). Modified syringe technique to prepare platelet rich plasma from rat blood, its quantitative assessment, and evaluation of platelets stored at 4C to determine its suitability for homologous application. Journal of Veterinary and Animal Sciences, 56(1), 13–19. https://doi.org/10.51966/jvas.2025.56.1.13-19
- 33. Verma, P., Kumar, V., Rathore, B., Singh, R. K., & Mahdi, A. A. (2016). HYPOLIPIDEMIC ACTIVITY OF ALOE VERA IN HYPERLIPIDEMIC RATS. International Journal of Pharmacognosy, 3(4), 196–200. https://doi.org/10.13040/IJPSR.0975-8232.IJP.3(4).196-00
- 34. Wang, S., Kozai, M., Mita, H., Cai, Z., Masum, Md. A., Ichii, O., Takada, K., & Inaba, M. (2021). REV-ERB agonist suppresses IL-17 production in γδT cells and improves psoriatic dermatitis in a mouse model. Biomedicine & Pharmacotherapy, 144, 112283. https://doi.org/https://doi.org/10.1016/j.biopha.2021.112283
- 35. Wong, K. C. (2015). Review of Spectrometric Identification of Organic Compounds, 8th Edition. Journal of Chemical Education, 92, 1602–1603. https://api.semanticscholar.org/CorpusID:101239903